Journal of Sound and Vibration (1997) **208**(2), 243–269

THE PASSAGE THROUGH RESONANCE IN A CATENARY–VERTICAL CABLE HOISTING SYSTEM WITH SLOWLY VARYING LENGTH

S. KACZMARCZYK

Department of Mechanical Engineering, University of Natal, Durban 4014, *Republic of South Africa*

(*Received* 31 *October* 1996, *and in final form* 4 *June* 1997)

A passage through resonance in a catenary–vertical cable system with periodic external excitation is analyzed. Due to the time-varying length of the vertical cable the natural frequencies of the system vary slowly, and a transient resonance may occur when one of the frequencies coincides with the frequency of an external excitation at some critical time. A simplified model of the system with proportional damping is proposed. This model is analyzed by using a combined perturbation and numerical technique. The method of multiple scales is used to formulate a uniformly valid perturbation expansion for the response near the resonance, and a system of first order ordinary differential equations for the slowly varying amplitude and phase of the response results. This system is integrated numerically on a slow time scale. A model example is discussed, and the behavior of the essential dynamic properties of the system during the transition through resonance is examined.

1. INTRODUCTION

Cables are widely used to carry payloads in vertical and inclined transport systems. In industrial hoisting arrangements a payload-carrying cable often consists of a horizontal or inclined catenary section and of a vertical section. In the mining industry for example, a typical design of a hoist system comprises a winder drum, a single cable and a conveyance. In this design, the cable passes from the drum over a sheave mounted in a headgear to the conveyance in a vertical shaft. Thus, the cable between the winder drum and the sheave forms a catenary, and the remaining part hanging below the headsheave forms the vertical rope. The entire cable translates axially and the vertical rope has a time-varying length.

In such arrangements the cable, due to its flexibility, is susceptible to vibration. Three major types of vibration may occur; namely, longitudinal, transverse, and torsional. These vibrations are caused by various sources of excitation. A load due to the winding cycle acceleration/deceleration profile is the most significant in the longitudinal transient response. A mechanism applied on the winder drum surface in order to achieve a uniform coiling pattern forms the primary source of stationary periodic excitation during the constant velocity winding phase for both the longitudinal and the transverse response. The torsional response is coupled with the longitudinal response, and occurs in triangle strand rope, which is known to respond in torsion to applied axial loads. During the wind the system parameters are changing due to the time-varying length of the cable. However, the rate of variation of the length is slow, and the oscillations represent waves in a slowly varying domain. Hence, the hoisting cable is essentially a nonstationary oscillatory system

0022–460X/97/470243 + 27 $25.00/0/sv971220

with slowly varying frequencies and mode shapes. Therefore, a passage through resonance may occur during the wind when one of the slowly varying frequencies coincides with the frequency of the periodic excitation at some critical time instant.

The study of vibration problems in hoisting cables has attracted wide attention. Savin and Goroshko [1, 2] analyzed a motion of a hoisting cable with slowly varying length using integro-differential equations, and taking into account a slip of the cable on the winder drum. Kotera [3] considered the longitudinal dynamics of a lift model and proposed a method to determine analytically a free and forced vibration response of a lift cable via a suitable transformation of variables. Greenway [4] analyzed the influence of physical parameters of a mine hoisting system on the dynamic longitudinal response using an analytical approach. Mankowski [5] investigated the non-linear dynamic behavior of mine hoisting cables, taking into account both longitudinal and lateral motions. Various mathematical models were developed, and the system was studied through an extensive computer simulation of the forced response of the system. The results of the simulation were correlated with measurements made on industrial installations. Constancon [6] extended this study by an analytical stationary analysis of the system stability, validated by laboratory experiment. The non-linear coupling between the catenary and the vertical system was accounted for in this analysis. An intensive numerical simulation of a non-stationary model of the system, intended to be used as a final validation, was also performed. Kumaniecka and Niziol [7] investigated the longitudinal–transverse vibration of a hoisting cable. The cable material non-linearity was taken into account and unstable regions were identified by applying the harmonic balance method.

Perturbation techniques can be used to study slowly varying oscillatory systems. Mitropolsky [8] established fundamental concepts in this field and developed an asymptotic method to analyze non-stationary oscillations in systems with slowly varying parameters. This method was further developed and modified by Agrawal and Ewan-Iwanowski [9] and Evan-Iwanowski [10]. Nayfeh [11] proposed the generalized multiple scales method to deal with the problem. Kevorkian [12, 13] used the multiple scales method and averaging techniques for systems with slowly varying parameters.

Perturbation methods present a useful tool in investigation of resonances. The phenomenon of passage through resonance in a hoisting cable system, referred to as transient resonance [14], is studied in this paper. A general mathematical model describing vibrations of one-dimensional distributed systems with slowly varying length is presented. A simplified longitudinal model of the catenary–vertical hoisting cable system with a periodic excitation is formulated in order to analyze the passage through resonance during the constant velocity winding phase. The first order approximation of the system response is determined by a combined numerical and analytical technique. The generalized method of multiple scales is applied to represent a uniformly valid perturbation expansion for the response near the resonance. This leads to a system of first order autonomous ordinary differential equations for the slowly varying amplitude and the phase of the response which is solved numerically.

2. VIBRATIONS OF ONE-DIMENSIONAL DISTRIBUTED SYSTEMS WITH A SLOWLY VARYING LENGTH

Forced oscillations of a one-dimensional distributed system with a time-varying length, and carrying concentrated inertia elements at intermediate and end-points, can be described by the equation

$$\rho(x)\ddot{u}(s,t) + \mathscr{L}[u(s,t)] + \mathscr{C}[\dot{u}(s,t)] = F(s,t,\theta), \qquad s \in D(t), \quad 0 \leqslant t < \infty, \tag{1}$$

where u is a deflection, dots designate partial derivative with respect to time, $\mathscr{L}$ is a linear spatial operator, $\mathscr{C}$ is a damping operator, F is a forcing function with a harmonic term of frequency $\dot{\theta} = \Omega$ and ρ is a mass distribution function. The spatial domain D is time-dependent, and is defined as

$$D(t) = \{s: l_1(t) < s < l_2(t)\}. \tag{2}$$

The time-varying length of the system is given as $L(t) = l_2(t) - l_1(t)$. When the variation of L, and therefore also the variation of the parameters l_i, $i = 1, 2$, is small over a time interval corresponding to the fundamental frequency of the system considered at fixed values of these parameters, the length is said to vary slowly with time [1]. The variation of l_i is then observed on a slow time scale defined as $\tau = \varepsilon T$, where T is a non-dimensional fast time scale, and ε is a small parameter. Therefore, the spatial domain is represented as $D = D(\tau)$, with $l_i = l_i(\tau)$, $i = 1, 2$. Consider the linear variation case when $l_i = l_{i0} + v_i t$, $i = 1, 2$, where $v_i =$ constant denotes the slow rate of variation of l_i. In order to represent the slow variability of l_i, one can introduce first a non-dimensional fast time scale $T = \omega_0 t$, where ω_0 is the initial fundamental frequency of the system. Upon assuming that $v_1 < v_2$, the small parameter ε can be defined then as

$$\varepsilon = v_1/\omega_0 L_0, \tag{3}$$

where $L_0 = l_{20} - l_{10}$ represents the initial length of the system, and $0 < \varepsilon \ll 1$. The parameters l_i, $i = 1, 2$, are then expressed in terms of a slow time τ as

$$l_1(\tau) = l_{10} + L_0\tau, \qquad l_2(\tau) = l_{20} + \frac{v_2}{v_1} L_0\tau. \tag{4}$$

The deflection u is subject to the homogeneous boundary conditions

$$B_1[u(s, t)] = 0, \quad \text{at } s = l_1(\tau), \qquad B_2[u(s, t)] = 0, \quad \text{at } s = l_2(\tau), \tag{5}$$

where B_1 and B_2 are linear spatial differential operators. The concentrated inertia elements can be accommodated in the equation of motion (1) as applied inertial loads so that the mass distribution function is given as

$$\rho(s) = m + \sum_{i=1}^{p} M_i\, \delta(s - L_i), \tag{6}$$

where m denotes the mass per unit length of the base structure, M_i is the magnitude of the ith concentrated inertia element located at $s = L_i$, and δ is the Dirac delta function.

The Rayleigh–Ritz procedure can be used to analyze the response of non-stationary systems with slowly varying parameters [2]. An approximate solution to the problem defined by the system (1), (5) can be represented by the expansion

$$u = \sum_{n=1}^{N} Y_n(s, \tau) q_n(t), \tag{7}$$

where q_n are generalized co-ordinates, and Y_n are slowly varying normal free-oscillation modes of the corresponding undamped stationary system with the inertia elements. They are solutions of

$$\mathscr{L}[Y_n(s, l_1, l_2)] = \omega_n^2(l_1, l_2)\rho(s) Y_n(s, l_1, l_2), \qquad x \in D,$$
$$B_1[Y_n(s, l_1, l_2)] = 0, \quad \text{at } s = l_1, \qquad B_2[Y_n(s, l_1, l_2)] = 0, \quad \text{at } s = l_2, \tag{8}$$

where ω_n are the natural frequencies of the system, considered at fixed values of l_1 and l_2.

By substituting the expansion (7) into equation (1), multiplying the result by Y_k, integrating over the domain D, using the boundary conditions (5), a second order ordinary differential equation system for the generalized co-ordinates is obtained. By using a fast non-dimensional time scale T, and a slow time scale τ, and noting also that $\dot{l}_i = \omega_0 \varepsilon \, \mathrm{d}l_i/\mathrm{d}\tau$, $i = 1, 2$, this system may be written in the form

$$\mathrm{d}^2 q_k/\mathrm{d}T^2 + \tilde{\omega}_k^2(\tau) q_k = \varepsilon \Gamma_k(T, \tau, \Omega, q_1, \ldots, q_N, \mathrm{d}q_1/\mathrm{d}T, \ldots, \mathrm{d}q_N/\mathrm{d}T) + Q(\varepsilon^2),$$
$$k = 1, 2, \ldots, N. \tag{9}$$

where $\tilde{\omega}_k = \omega_k/\omega_0$ and Γ_k are functions containing terms which represent the excitation due to the non-stationary nature of the system, the external periodic excitation and the damping in the system.

In order to generate an approximate solution, the slowly varying oscillatory second order system of N equations (9) can be transformed into a Hamiltonian standard form of $2N$ first order differential equations in terms of action-angle variables [13]. Later, perturbation techniques, namely the method of averaging or the method of multiple scales, can be applied to determine the solution. Alternatively, these techniques can be applied directly to the second order model. By using the method of multiple scales a first order system can be obtained to compute the amplitudes and the phases for the first approximation of the response. In this procedure, the following form of the solution is assumed [15],

$$q_k = \sum_{j=0}^{M} \varepsilon^j q_{kj}(\phi_k, \tau) + O(\varepsilon^{M+1}), \tag{10}$$

where ϕ_k represents a fast scale and is defined as

$$\phi_k = \int_0^t \omega_k(\varepsilon\xi) \, \mathrm{d}\xi. \tag{11}$$

By substituting the expansion (10) into equation (9) and equating coefficients of the same power of ε, one obtains a set of differential equations for the approximations q_{kj}, $j = 0, 1, \ldots, M$. These equations are solved in succession by using the solvability conditions that make the expansion (10) uniform.

The longitudinal dynamics of hoisting cable systems can be described by a differential equation of the type given by equation (1), and analyzed as discussed above. The dynamic model of a hoisting cable system with periodic excitation is presented in what follows. Hamilton's principle is applied to derive the equation of motion, with the cable damping mechanism represented by an equivalent viscous damping model.

3. DYNAMIC MODEL OF A HOISTING CABLE SYSTEM

The model of a hoisting cable system is represented in Figure 1. In this model, the cable is divided into a horizontal catenary of length $OC = L_c$ passing over a sheave of radius R, and of mass moment of inertia I, and into a vertical rope with a mass M, representing the conveyance with payload, attached to its bottom end. The end O_1 of the cable is moving with a prescribed winding velocity $v(t)$ due to the cable being coiled onto a rotating cylindrical drum, so that the entire system translates axially, with the mass M being constrained in a lateral direction. The section $l = OO_1$ represents a varying length of this

part of the cable that is already coiled onto the winder drum. The cable has a constant effective cross-sectional area A, a constant mass per unit length m and effective Young's modulus E.

Upon assuming that the modulus E of the cable material is high the strain of the cable wound around the drum can be neglected [2], and the length l is then given by

$$l(t) = l(0) \pm \int_0^t v(\xi)\, \mathrm{d}\xi, \tag{12}$$

where the signs + and − correspond to ascending and descending, respectively, and $l(0)$ is the initial length. The length l, and therefore also the length of the vertical rope, is assumed to vary slowly, and its variation will be observed on a separate slow time scale as discussed in the preceding section. It is assumed that there is no cable slip on the drum or across the sheave. Only longitudinal motions of the cable are considered, with the lateral and torsional displacements being ignored. The damping forces at the sheave and at the conveyance are neglected.

In order to describe the longitudinal oscillations of the cable the classical moving frame approach is applied [16]. Two frames of reference are established: a co-ordinate system $O_1\bar{x}\bar{y}$ attached to and moving with the upper end of the cable, and a stationary inertial system OXY. The dynamic deformed position P of an arbitrary section of the cable during its motion is defined in the inertial frame by the vector

$$\mathbf{X}(s, t) = \mathbf{X}_{O_1}(t) + \bar{\mathbf{x}}(s, t), \tag{13}$$

with

$$\bar{\mathbf{x}}(s, t) = \bar{\mathbf{x}}^i(s) + \bar{\mathbf{U}}(s, t), \tag{14}$$

where $\mathbf{X}_{O_1} = [-l(t), 0]$ defines the position of the origin O_1 in the inertial frame, $\bar{\mathbf{x}}^i = [s, 0]$ defines the initial position P^i of the cable section, $\bar{\mathbf{U}} = [\bar{u}(s, t), 0]$ represents the dynamic displacement vector, and s denotes the Lagrangian (material) co-ordinate identifying the cable section in the initial state, and measured from the origin O_1. The upper bar denotes vectors referred to the moving frame. In this formulation the axial transport motion is treated as an overall rigid body translation, with the dynamic elastic deformations being referred to the moving frame. The entire cable is therefore prestressed in its initial reference (dynamically undeformed) state during its transport motion, with the mean catenary tension slowly varying with time due to the slowly varying length of the vertical rope. All

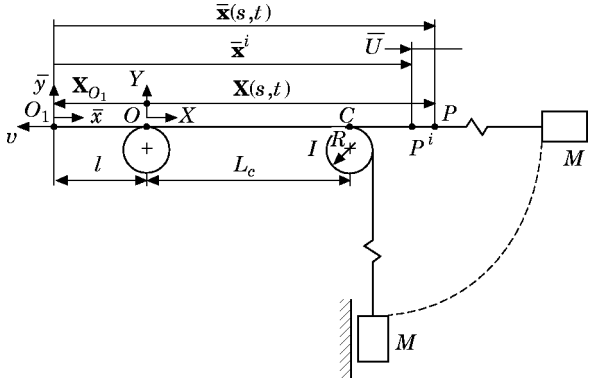

Figure 1. The model of a catenary–vertical cable system.

of the dynamic characteristics of the cable are functions of the independent variables (s, t), where the material co-ordinate s is referred to the prestressed reference configuration, and to the moving frame. With the dynamic deflection in the catenary and the vertical cable denoted as u_c and u, respectively, the deformed position vector $\mathbf{X}$ is given as

$$\mathbf{X} = \begin{Bmatrix} \mathbf{X}_c = [s + u_c(s, t) - l, 0], & l \leqslant s \leqslant L_1 \\ \mathbf{X}_v = [s + u(s, t) - l, 0], & L_1 \leqslant s \leqslant L_0 \end{Bmatrix}, \tag{15}$$

where $L_1 = l + L_c$, and L_0 denotes the total length of the cable in the reference state. The continuity of deflection across the sheave requires $u_c(L_1, t) = u(L_1, t) = u_1$. The co-ordinate $u_2 = u(L_0, t)$ represents the dynamic elastic deflection at the cable bottom end. The velocity vector of a cable particle P can be expressed as

$$\mathbf{V}(s, t) = \frac{\mathrm{d}\mathbf{X}}{\mathrm{d}t} = \begin{Bmatrix} \mathbf{V}_c = [\dot{u}_c(s, t) - \dot{l}, 0], & l \leqslant s \leqslant L_1 \\ \mathbf{V}_v = [\dot{u}(s, t) - \dot{l}, 0], & L_1 \leqslant s \leqslant L_0 \end{Bmatrix}, \tag{16}$$

The equations governing the longitudinal response of the system can be derived by applying the approach developed by Perkins and Mote [17] in their theory of travelling elastic cables. In this approach, Hamilton's principle is used, which requires

$$\int_{t_1}^{t_2} (\delta E - \delta \Pi_e - \delta \Pi_g + \delta W_{nc})\, \mathrm{d}t = 0, \tag{17}$$

where E, Π_e, and Π_g denote the system kinetic energy, the cable elastic strain energy, and the system gravitational potential energy, respectively, and δW_{nc} represent the virtual work of the damping forces. Upon assuming that dynamic deflections of section OO_1 of the cable can be neglected, the kinetic energy of the system is expressed as

$$E(\dot{u}_c, \dot{u}, \dot{u}_1, \dot{u}_2) = \tfrac{1}{2} \int_l^{L_1} m\mathbf{V}_c \cdot \mathbf{V}_c \,\mathrm{d}s + \tfrac{1}{2} \int_{L_1}^{L_0} m\mathbf{V}_v \cdot \mathbf{V}_v \,\mathrm{d}s + \tfrac{1}{2} \frac{I}{R^2} \dot{q}_1^2 + \tfrac{1}{2} M \dot{q}_2^2, \tag{18}$$

where $\dot{q}_1 = \dot{u}(L_1, t) - \dot{l}$, and $\dot{q}_2 = u(L_0, t) - \dot{l}$, with q_1 and q_2 representing the total displacements at the sheave and at the conveyance, respectively.

The elastic strain energy of the cable is

$$\Pi_e(\varepsilon_c, \varepsilon) = \Pi_e^i + \int_l^{L_1} (T_c^i + \tfrac{1}{2} EA\varepsilon_c)\varepsilon_c \,\mathrm{d}s + \int_{L_1}^{L_0} (T^i + \tfrac{1}{2} EA\varepsilon)\varepsilon \,\mathrm{d}s, \tag{19}$$

where ε_c and ε represent the strain measure in the catenary section and the vertical section of the cable respectively, Π_e^i is the strain energy in the initial state, and T_c^i and T^i represent the tension in the catenary and vertical rope in the initial state respectively. It is assumed that both rotations and displacements in the catenary cable are small, and only longitudinal motions result in the vertical cable. Hence, the strain measures are given in the classical linear form, as for a straight bar, by

$$\varepsilon_c = u_{c_s}, \qquad \varepsilon = u_s, \tag{20, 21}$$

where $(\,)_s$ denotes partial differentiation with respect to s.

The gravitational potential energy of the cable expressed in terms of the dynamic deflections is given by

$$\Pi_g(u, u_2) = \Pi_g^i - \int_{L_1}^{L_0} mgu \, \mathrm{d}s - Mgq_2, \tag{22}$$

where Π_g^i is the gravitational potential energy in the initial equilibrium configuration.

The virtual work due to the damping forces can be expressed as

$$\delta W_{nc} = \int_{l}^{L_1} F_c \delta u_c \, \mathrm{d}s + \int_{L_1}^{L_0} F_v \delta u \, \mathrm{d}s, \tag{23}$$

where F_c and F_v represent the catenary and the vertical cable distributed damping forces, respectively.

Substituting equations (18–22) into Hamilton's principle (17) yields the following system of equations for the deflection:

$$m(\ddot{u}_c - \ddot{l}) - EA\varepsilon_{c,s} - T^i_{c,s} - F_c = 0, \qquad l < s < L_1, \tag{24}$$

$$m(\ddot{u} - \ddot{l}) - EA\varepsilon_{,s} - T^i_{,s} - F_v - mg = 0, \qquad L_1 < s < L_0, \tag{25}$$

$$(I/R^2)[\ddot{u}(L_1, t) + \dot{u}_{,s}(L_1, t)\dot{l} - \ddot{l}] + EA\varepsilon_c(L_1, t) - EA\varepsilon(L_1, t) + T^i_c(L_1) - T^i(L_1) = 0, \tag{26}$$

$$M[\ddot{u}(L_0, t) - \ddot{l}] + EA\varepsilon(L_0, t) + T^i(L_0) - Mg = 0. \tag{27}$$

In this system equations (24 and 25) describe the dynamics of the catenary and vertical rope respectively, equation (26) represents the balance of forces across the sheave, and the final equation (27) defines motion of the end mass.

The equations of the initial equilibrium can be extracted from the system (24–27) by setting all time derivatives and the dynamic strain components to zero. The following conditions result:

$$T^i_{c,s} = 0, \qquad T^i_{,s} + mg = 0, \qquad T^i_c(L_1) = T^i(L_1), \qquad T^i(L_0) = Mg. \tag{28}$$

Using the first equilibrium condition, and neglecting the inertia and the catenary damping forces in (24) yields the relationship

$$u_{c,s} = e(t), \tag{29}$$

where $e(t)$ represents the spatially uniform catenary longitudinal elastic strain. Equation (29) can be integrated over the domain $l < s < L_1$, which yields

$$e(t) = (1/L_c)[u_1 - u_c(l, t)]. \tag{30}$$

In order to define the boundary condition $u_c(l, t)$, it is relevant to consider a mechanism employed to implement the coiling process. Typically, a repetitive coiling pattern during a winding cycle in hoist systems is achieved via a symmetrical 180° Lebus liner [5]. In this mechanism the winder drum surface is covered by parallel circular grooves with two diametrically opposed crossover zones per drum circumference, as shown in Figure 2. Each zone offsets the grooves by half a cable diameter and when the cable passes through a crossover an additional axial displacement relative to the nominal transport motion occurs. The magnitude of this displacement is calculated as the difference between the arc length traversed through the crossover and the corresponding diametrical arc [6]

$$u_0 = \sqrt{(R_d\alpha)^2 + d^2/4} - R_d\alpha, \tag{31}$$

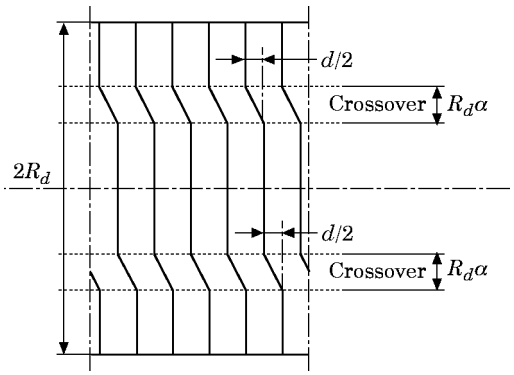

Figure 2. The crossover zones of a Lebus liner.

where R_d is the drum radius, d represents the cable diameter and α is the angle defining the diametrical arc corresponding to the crossover region. As the crossover occurs twice per drum revolution, a periodic boundary excitation results that can be represented by the boundary condition

$$u_c(l, t) = u_0 \cos \Omega t, \tag{32}$$

where $\Omega = 2v/R_d$.

Treating the sheave and the end mass M as additional inertial loads applied to the system, and using the equilibrium conditions (28) yields the dynamic model of the hoisting cable system,

$$\rho(s)\ddot{u} - EAu_{,ss} = \rho(s)\ddot{l} - [M_S\dot{u}_{,s}i + EAe(t)]\,\delta(s - L_1) + F_v, \qquad L_1^- < s < L_0^+, \quad 0 \leqslant t < \infty, \tag{33}$$

with homogeneous boundary conditions

$$EAu_{,s}(L_1^-, t) = 0, \qquad EAu_{,s}(L_0^+, t) = 0, \tag{34, 35}$$

where $M_S = I/R^2$ is the effective mass of the sheave, $e(t)$ is given by equation (30) together with equation (32), L_1^- denotes the point immediately to the left of M_S, L_0^+ is the point immediately to the right of M, and the mass distribution function ρ is defined as

$$\rho(s) = m + M_S\,\delta(s - L_1) + M\,\delta(s - L_0). \tag{36}$$

Thus, in this formulation the system is essentially regarded as being free at the ends $s = L_1^-$, and $s = L_0^+$, respectively. The parameter l is time-dependent, and is assumed to vary slowly. This condition agrees well with nominal parameters of a winding cycle in most industrial hoist systems. Therefore, a separate slow time scale τ can be chosen to observe the parameter variation so that $l = l(\tau)$, as indicated earlier.

4. DAMPING MODEL

Damping forces in hoisting cables, which are steel wire ropes, are complex, and would likely arise from inter-strand viscous and Coulomb friction, and from internal friction in separate wires. It is difficult to define correctly the exact damping mechanism in wire ropes. However, it is a recognized practice to replace resisting forces of a complicated nature by equivalent viscous damping for purposes of analysis [18]. The equivalent damping

coefficient can be then determined through an experiment. For example, Vanderveldt *et al*. [19] identified the equivalent viscous damping coefficient in a wire rope system from measurements of the logarithmic decrement. This approach has been successfully applied in the formulation of simulation models used in the mining industry [20].

The viscous damping distributed force in the cable can be given in the form

$$F_v = -\mathscr{C}[\dot{u}], \tag{37}$$

where $\mathscr{C}$ is a linear operator. The special case of viscous damping known as proportional damping has the advantage of being particularly convenient to analyze. In this case the operator $\mathscr{C}$ is a linear combination of the stiffness operator $\mathscr{L}$ and of the mass distribution function ρ, and is given as

$$\mathscr{C} = \mu_1 \mathscr{L} + \mu_2 \rho, \tag{38}$$

where μ_1 and μ_2 are coefficients of damping. For this particular model, when the modal analysis is applied the modal damping ratio defined as

$$\varsigma_n = \tfrac{1}{2}(\mu_1 \omega_n + \mu_2/\omega_n), \tag{39}$$

where ω_n is the nth natural frequency, represents the damping effect on the nth mode. When $\mu_2 = 0$ the resulting damping model is referred to as relative damping. In this case the damping ratio in each mode is proportional to the corresponding natural frequency, which means that the responses of the higher modes will be more rapidly damped than those of the lower modes. As in general the fundamental mode dominates the longitudinal response of a hoisting cable, the relative damping model can be assumed as being intuitively appropriate to represent the overall damping effect in the system. When this approach is used the damping coefficient μ_1 is usually assumed to be a function of some cable parameters, which must be established from an appropriate experiment. Savin and Goroshko [2] assumed relative damping in their analysis of oscillations in mine hoist cables. It was shown that the coefficient μ_1 is independent of the amplitude of oscillations in the cable dynamic tension, but depends on the mean (static) value of the cable tension: namely, μ_1 decreases with increasing mean tension. This effect was also observed by Mankowski and Cox [21]. It can be argued that when the tension is increased, the wire strands are more readily locked, and the inter-strand relative motion is constrained, resulting in the coefficient μ_1 being decreased. This agrees with an earlier observation by Vanderveldt and Gilheany [22] who found that the speed of propagation of a longitudinal pulse in wire ropes increases with increasing applied tension load, and postulated that this was due to the cable approaching the geometry of a solid bar due to a gradual tightening together the wires and strands. Greenway [4] also proposed the relative damping model, and extracted the damping coefficient from the measurement of the logarithmic measurement of the fundamental longitudinal mode performed on a mine hoist installation. It was shown that the damping coefficient increased in proportion to the rope length. Constancon [6] analyzed the results of damping measurements via drop tests carried out at Elandsrand Mine, RSA. In these tests a conveyance was clamped between the guides, loaded with a dead weight, and released. The response was monitored with an accelerometer, and the modal damping ratios were extracted from the measurements by using standard parameter estimation procedures. A strong dependency of the fundamental mode ratio on the mean rope tension was recorded. It was evident that the damping ratio decreased approximately linearly with the tension. However, it was decided to adopt the general proportional model and to determine the coefficients μ_1 and μ_2 by globally fitting the fundamental mode ratio data to the model, thus ignoring the dependence on the mean tension. In this approach the relative damping coefficient μ_1 was assumed to depend on

the cable length, as proposed by Greenway. The coefficient μ_2 was taken as a constant estimated from the global fit, in order to account for, in an average manner, the lower damping in the higher modes.

In the present analysis the main concern is to formulate a simple but efficient model of a hoisting cable system, and to use this model to simulate the passage through resonance which may occur during the wind. This model is to adequately account for the fundamental features of the real system, and is to be based on the assumption that the fundamental mode dominates the longitudinal response of the system. Therefore, in this approach the equivalent relative viscous damping model is adopted to represent the overall damping effort in the system. In this model the dependency of the damping coefficient μ_1 on the mean tension is accommodated, as proposed by Savin and Goroshko [2]. In this approach, based on experimental data, the damping coefficient is defined as

$$\mu_1 = 10^{-4}\left(0{\cdot}5 + \frac{23\,000}{3500 + 0{\cdot}75 \times 10^{-5}\sigma^i}\right), \tag{40}$$

where σ^i denotes the mean stress in the cable in N/m^2 and is given as

$$\sigma^i = T^i/A, \tag{41}$$

with the mean (static) tension in the vertical rope determined from the equilibrium conditions (28) and given as

$$T^i = Mg + mg(L_0 - s). \tag{42}$$

Therefore, the coefficient μ_1 depends on the material co-ordinate s, and the damping operator for the hoisting cable model is given by

$$\mathscr{C} = -\mu_1(s)EA\,\partial^2/\partial s^2. \tag{43}$$

Substituting the damping operator (43) into equation (37), and using the result (33), yields the equation governing the longitudinal response of the system:

$$\rho(s)\ddot{u} - EAu_{,ss} - EA\mu_1(s)\dot{u}_{,ss} = \rho(s)\ddot{l} - [M_S\dot{u}_{,s}\dot{l} + EAe(t)]\,\delta(s - L_1), \qquad L_1^- < s < L_0^+,$$
$$0 \leqslant t < \infty. \tag{44}$$

5. DISCRETE MODEL

The discrete model can be determined from equations (44, 34, and 35) through application of the expansion defined by equation (7). When a single term is taken in this expansion, the result is referred to as a single-mode approximation, and the system is reduced to a single-degree-of-freedom model. This simple model has been used extensively and successfully in the analysis of free and forced vibrations of structures [23]. The above approach also can be applied to investigate the longitudinal vibration and resonance in the hoisting cable system. This vibration is referred to, colloquially, as "yo-yo" type oscillation of the vertical cable and the conveyance [24]. The resulting oscillation is of large amplitude and of low frequency, and it is reasonable to conclude that the shape of the vibration is close to the fundamental normal mode of the system. The resonance is then understood as coincidence of the slowly varying natural fundamental frequency $\omega_r = \omega_r(l)$ with the forcing frequency Ω at some critical time instant.

The single-mode approximation is assumed as

$$u = Y_r(s, l)q_r(t), \tag{45}$$

where

$$Y_r(s, l) = \cos \gamma_r z(s, l) - (M_S/m)\gamma_r \sin \gamma_r z(s, l) \tag{46}$$

is the fundamental elastic free oscillation mode of the corresponding unconstrained system with l being fixed, as shown in Figure 3, with $\gamma_r = \omega_r(l)/c$, where $c = \sqrt{EA/m}$, and $z = s - L_1$. The slowly varying parameter γ_r is determined from the frequency equation

$$\frac{M_S}{m}\gamma_r\left(\cos \gamma_r L_v - \frac{M}{m}\gamma_r \sin \gamma_r L_v\right) + \frac{M}{m}\gamma_r \cos \gamma_r L_v + \sin \gamma_r L_v = 0, \tag{47}$$

where $L_v = L_0 - L_1$. The details of the eigenvalue problem solution for the unconstrained system of Figure 3 are given in Appendix D.

The representation (45) results in the following expressions for partial derivatives of u:

$$\ddot{u} = ((\partial^2 Y_r/\partial l^2)\dot{l}^2 + (\partial Yr/\partial l)\ddot{l})q_r + 2(\partial Y_r/\partial l)\dot{l}\dot{q}_r + Y_r\ddot{q}_r,$$
$$u_{,ss} = Y_{r,ss}q_r, \qquad \dot{u}_{,s} = (\partial Y_{r,s}/\partial l)\dot{l}q_r + Y_{r,s}\dot{q}_r. \tag{48}$$

By substituting equations (48) into equation (44), multiplying the result by Y_r, integrating from L_1 to L_0, accounting for the boundary conditions (34 and 35), using equation (30), and noting that

$$Y_r(L_1, l) = 1, \qquad Y_{r,s}(L_1, l) = -(M_S/m)\gamma_r^2, \qquad (\partial Y_{r,s}/\partial l)(L_1, l) = \gamma_r\left(\gamma_r - 2\frac{M_S}{m}\frac{\mathrm{d}\gamma_r}{\mathrm{d}l}\right), \tag{49}$$

the following system results:

$$\ddot{q}_r + \bar{\omega}_r^2(l)q_r = \frac{1}{m_r(l)}\left[EAg_{rr}(l) - 2\dot{l}c_{rr}(l) + \frac{M_S^2}{m}\dot{l}\gamma_r^2(l)\right]\dot{q}_r$$
$$- \frac{1}{m_r(l)}\left[\ddot{l}c_{rr}(l) - EA\dot{l}b_{rr}(l) + \dot{l}^2 d_{rr}(l) + M_S\dot{l}^2\gamma_r\left(\gamma_r - 2M_S\frac{\mathrm{d}\gamma_r}{\mathrm{d}l}\right)\right]q_r$$
$$+ \frac{e_r(l)}{m_r(l)}\ddot{l} + K_r(l)\cos \Omega t, \tag{50}$$

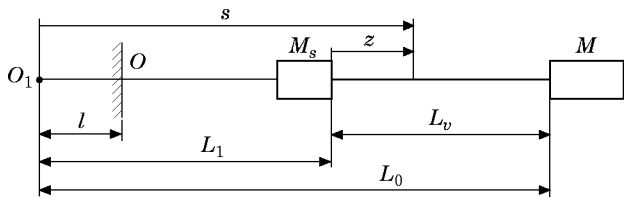

Figure 3. The unconstrained model of the hoisting system.

where

$$\bar{\omega}_r^2 = \omega_r^2(l) + \frac{1}{m_r(l)}\frac{EA}{L_c}, \qquad K_r = \frac{1}{m_r(l)}\frac{EA}{L_c}u_0, \tag{51, 52}$$

with the coefficients m_r, b_{rr}, c_{rr}, d_{rr}, e_r and g_{rr} being defined in Appendix A.

Two time scales are defined in order to seek the solution of equation (50). The first one, a fast non-dimensional scale, is determined as

$$T = \bar{\omega}_0 t, \tag{53}$$

where $\bar{\omega}_0 = \bar{\omega}_r(l(0))$. The second scale is a slow scale, $\tau = \varepsilon T$, and a variation of l is observed on this scale. For example, during the ascending constant velocity winding phase, following the relation (12), this length is given as

$$l = l(0) + v_c t, \tag{54}$$

where v_c denotes the nominal winding velocity. Assuming $l(0) = 0$, and defining the small parameter ε according to the relationship (3) as

$$\varepsilon = v_c/\bar{\omega}_0 L_0, \tag{55}$$

yields

$$l = L_0\tau. \tag{56}$$

Using the fast and slow scales in (50), with ε defined by (55), and assuming that the damping is small, so that one may set $\mu_1 = \varepsilon\mu_1^*$, yields the equation

$$\frac{\mathrm{d}^2 q_r}{\mathrm{d}T^2} + \tilde{\omega}_r^2(\tau)q_r = \varepsilon f_r\left(\tau, \frac{\mathrm{d}q_r}{\mathrm{d}T}\right) + K_r(\tau)\cos\tilde{\Omega}T + O(\varepsilon^2), \tag{57}$$

where $\tilde{\omega}_r = \bar{\omega}_r/\bar{\omega}_0$, $\tilde{\Omega} = \Omega/\bar{\omega}_0$, and

$$f_r\left(\tau, \frac{\mathrm{d}q_r}{\mathrm{d}T}\right) = \frac{1}{m_r(\tau)}\left[EA\frac{L_0}{v_c}g_{rr}(\tau) - 2l'c_{rr}(\tau) + \frac{M_S^2}{m}l'\gamma_r^2(\tau)\right]\frac{\mathrm{d}q_r}{\mathrm{d}T}, \tag{58}$$

where the prime denotes the derivative with respect to τ.

6. THE MULTIPLE SCALES SOLUTION

Following the expansion (10), the solution is sought in terms of the fast and slow scales in the form

$$q_r = q_{r0}(\phi_r, \tau) + \varepsilon q_{r1}(\phi_r, \tau) + O(\varepsilon^2), \tag{59}$$

where

$$\mathrm{d}\phi_r/\mathrm{d}T = \tilde{\omega}_r(\tau). \tag{60}$$

When $\tilde{\Omega}$ is away from $\tilde{\omega}_r(\tau)$ in the system (57) non-resonant oscillations occur, and the effect of the external excitation is small unless its amplitude is large: that is, $K_r = O(1)$. However, one is more concerned with the resonant case, when values $\tilde{\omega}_r(\tau)$ are near $\tilde{\Omega}$.

This nearness can be quantified by a slowly varying detuning parameter $\sigma_r(\tau)$, introduced as

$$\tilde{\Omega} - \tilde{\omega}_r(\tau) = \varepsilon\sigma_r(\tau). \tag{61}$$

Therefore, when the relationship (60) is taken into account, one obtains from equation (61)

$$\tilde{\Omega}T = \phi_r + \vartheta_r(\tau), \tag{62}$$

where

$$\vartheta_r(\tau) = \varepsilon \int_0^T \sigma_r(\varepsilon T)\, \mathrm{d}T. \tag{63}$$

When $\sigma_r = 0$, unbounded oscillations would be predicted for a corresponding system with constant parameters. In the actual system the oscillations are limited by the damping and influenced by the non-stationary terms on the right side of equation (57), present as components of the function (58). Therefore, the excitation needs to be ordered so that it will appear when the damping and the non-stationary terms appear. Thus, in order to determine the first approximation, one sets

$$K_r = 2\varepsilon k_r, \tag{64}$$

so that $K_r = O(\varepsilon)$. Substituting equation (59) into equation (57) and equating the coefficients of ε^0 and ε on both sides, yields

$$\tilde{\omega}_r^2\left(\frac{\partial^2 q_{r0}}{\partial \phi_r^2} + q_{r0}\right) = 0, \tag{65}$$

$$\tilde{\omega}_r^2\left(\frac{\partial^2 q_{r1}}{\partial \phi_r^2} + q_{r1}\right) = -2\tilde{\omega}_r \frac{\partial^2 q_{r0}}{\partial \phi_r\, \partial \tau} - \tilde{\omega}_r' \frac{\partial q_{r0}}{\partial \phi_r} + f_r\left(\tau, \tilde{\omega}_r \frac{\partial q_{r0}}{\partial \phi_r}\right) + 2k_r \cos \tilde{\Omega}T. \tag{66}$$

The details of this procedure are given in Appendix B.

The general solution of equation (65) is found to be

$$q_{r0} = A_r(\tau)\, \mathrm{e}^{\mathrm{i}\phi_r} + \overline{A}_r(\tau)\, \mathrm{e}^{-\mathrm{i}\phi_r}, \tag{67}$$

where $\overline{A}_r$ is the complex conjugate of A_r which is given by the polar form

$$A_r(\tau) = \tfrac{1}{2} a_r(\tau)\, \mathrm{e}^{\mathrm{i}\beta_r(\tau)}, \tag{68}$$

where a_r and β_r are real. Using equation (67) and (62) in equation (66), with $f_r(\tau, \tilde{\omega}_r\, \partial q_{r0}/\partial \phi_r)$ expanded in a Fourier series, one obtains

$$\tilde{\omega}_r^2\left(\frac{\partial^2_{q_{r1}}}{\partial \phi_r^2} + q_{r1}\right) = -\mathrm{i}(2\tilde{\omega}_r A_r' + \tilde{\omega}_r' A)\, \mathrm{e}^{\mathrm{i}\phi_r} + \sum_{n=-\infty}^{\infty} f_{rn}(A_r, \tilde{A}_r, \tau)\, \mathrm{e}^{\mathrm{i}n\phi_r} + k_r\, \mathrm{e}^{\mathrm{i}(\phi_r + \vartheta_r)} + cc, \tag{69}$$

where

$$f_{rn}(A_r, \overline{A}_r, \tau) = \frac{1}{2\pi} \int_0^{2\pi} f_r(A_r, \overline{A}_r, \tau, \phi_r)\, \mathrm{e}^{-\mathrm{i}n\phi_r}\, \mathrm{d}\phi_r, \tag{70}$$

and *cc* denotes the complex conjugate of the preceding terms. The condition for the elimination of the secular terms in equation (69) is

$$-\mathrm{i}(2\tilde{\omega}_r A_r' + \tilde{\omega}_r' A) + f_{r1}(A_r, \bar{A}_r, \tau) + k_r \, \mathrm{e}^{\mathrm{i}\vartheta_r} = 0, \tag{71}$$

where

$$f_{r1}(A_r, \bar{A}_r, \tau) = \frac{1}{2\pi} \int_0^{2\pi} f_r(A_r, \bar{A}_r, \tau, \phi_r) \, \mathrm{e}^{-\mathrm{i}\phi_r} \, \mathrm{d}\phi_r. \tag{72}$$

By expressing A_r in polar form, separating the result into its real and imaginary parts, and also denoting

$$\psi_r = \vartheta_r - \beta_r, \tag{73}$$

one obtains the set

$$a_r' = -\tfrac{1}{2}\frac{\tilde{\omega}_r'}{\tilde{\omega}_r} a_r - \frac{1}{2\pi\tilde{\omega}_r} \int_0^{2\pi} f_r(\tau, -a_r\tilde{\omega}_r \sin\theta_r) \sin\theta_r \, \mathrm{d}\theta_r + \frac{k_r}{\tilde{\omega}_r} \sin\psi_r,$$

$$\psi_r' = \sigma_r(\tau) + \frac{1}{2\pi\tilde{\omega}_r a_r} \int_0^{2\pi} f_r(\tau, -a_r\tilde{\omega}_r \sin\theta_r) \cos\theta_r \, \mathrm{d}\theta_r + \frac{k_r}{\tilde{\omega}_r a_r} \cos\psi_r, \tag{74}$$

where $\theta_r = \phi_r + \beta_r$. Using equation (58) in equations (74), leads to

$$a_r' = -\tfrac{1}{2}\left\{\frac{\tilde{\omega}_r'}{\tilde{\omega}_r} - \frac{1}{m_r(\tau)}\left[EA\frac{L_0}{v_c} g_{rr}(\tau) - 2l' c_{rr}(\tau) + \frac{M_S^2}{m} l' \gamma_r^2(\tau)\right]\right\} a_r + \frac{k_r}{\tilde{\omega}_r} \sin\psi_r,$$

$$\psi_r' = \sigma_r(\tau) + \frac{k_r}{\tilde{\omega}_r a_r} \cos\psi_r, \tag{75}$$

where $\tilde{\omega}_r'$, representing the derivative of the slowly varying frequency with respect to τ, is determined in Appendix C. Following the expansion (59), the first approximation to the solution is obtained when equation (73) together with equation (62) are used in equation (67). This results in

$$q_r = a_r \cos(\tilde{\Omega}T - \psi_r) + O(\varepsilon), \tag{76}$$

with a_r and ψ_r given by equations (75).

7. NUMERICAL EXAMPLE AND RESULTS

The system evolution through resonance can be analyzed through solving the set of equations (75). These are autonomous ordinary differential equations with variable coefficients to be determined numerically. For this non-stationary system steady state, solutions do not exist, and the response of the system is aperiodic. The equations (75) do not easily lend themselves to an analytical solution, and a numerical solution for the amplitude a_r and the phase γ_r is sought. The following system parameters have been assumed in calculations: $M = 17\,584$ kg, $I = 15\,200$ kg m^2, $m = 8{\cdot}4$ kg/m, $L_c = 74{\cdot}95$ m, $L_0 = 2174{\cdot}95$ m, $A = 0{\cdot}001028$ m^2, $E = 1{\cdot}1 \times 10^{11}$ N/m^2, $d = 0{\cdot}048$ m, $R = R_d = 2{\cdot}14$ m and $\alpha = 0{\cdot}2$ rad. A transition through fundamental resonance is investigated during the ascending cycle, when the frequency Ω of the excitation is near the slowly varying frequency $\bar{\omega}_r$ of the cable system, given by equation (51). The natural frequency ω_r is

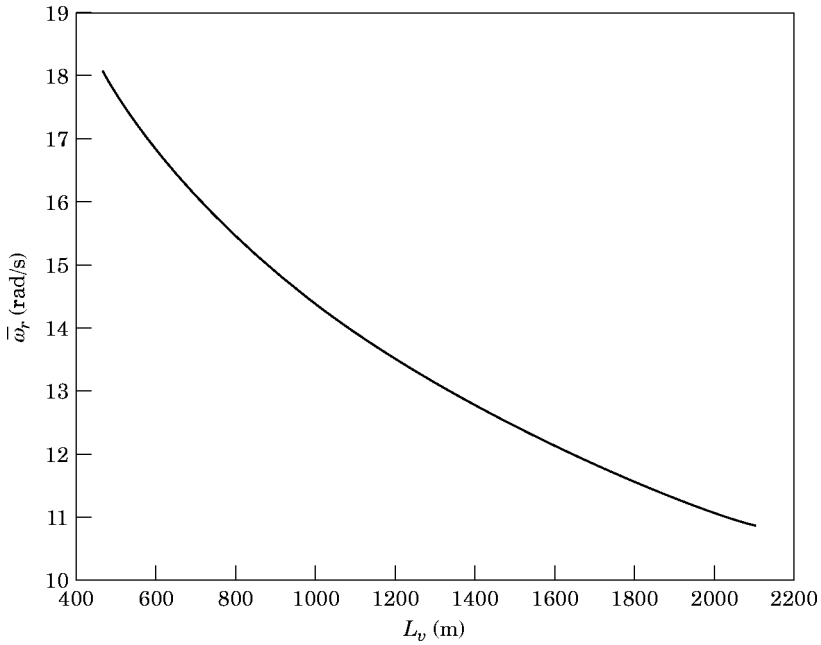

Figure 4. The slowly varying frequency $\bar{\omega}_r$ versus the vertical length.

computed from the transcendental equation (47), and $\bar{\omega}_r$ is plotted against the vertical length L_v in Figure 4. During the ascending constant velocity phase the length parameter l is given by equation (56), and the small parameter ε is defined by equation (55).

In order to determine the amplitude a_r and the phase ψ_r, the system (75) is integrated numerically by using MATLAB implementation of the Runge–Kutta method. The dynamic displacements can be then found from equation (45), together with equations (46) and (76). The time response plots at the sheave $u_S = Y_r(L_1, l)q_r(t)$, and at the conveyance $u_M = Y_r(L_0, l)q_r(t)$, are shown in Figure 5 for the winding velocity $v_c = 15$ m/s. In these plots the displacements are bounded by the envelopes formed by the amplitude curves. These vibration envelopes are of primary interest, and the corresponding envelope curves $a_S = Y_r(L_1, l)a_r$ and $a_M = Y_r(L_0, l)a_r$ for four winding velocities, namely $v_{c1} = 12$ m/s, $v_{c2} = 14$ m/s, $v_{c3} = 16$ m/s and $v_{c4} = 18$ m/s, are presented in Figure 6. The non-stationary frequency–response curves are shown in Figure 7, where the amplitude a_r is plotted against the detuning parameter σ_r. It can be seen that the resonance region is reached sooner for lower values of the winding velocity, while the detuning parameter σ_r decreases when making a single slow passage through zero. The amplitudes exhibit oscillatory behavior before the resonance, and near the resonance ($\sigma_r \approx 0$) the amplitudes increase rapidly and decline afterwards due to damping, developing damped beat phenomena. The period of the beats decreases with time. It can be noted that the lower the winding velocity, the higher the maximum value of the corresponding amplitude. For instance, for the velocity of 12 m/s the sheave amplitude reaches the maximum value of approximately 0·07 m shortly after the resonance, and for the velocities of 14, 16 and 18 m/s, the approximate maximum values are 0·045, 0·042 and 0·033 m, respectively.

The plots of the total catenary tension T_c, and of the total vertical cable tension T_S at the sheave and T_M at the conveyance against the vertical cable length L_v for the velocity $v_c = 15$ m/s are shown in Figure 8. The total catenary tension is calculated as

$$T_c(t) = T_c^i + EAe(t), \tag{77}$$

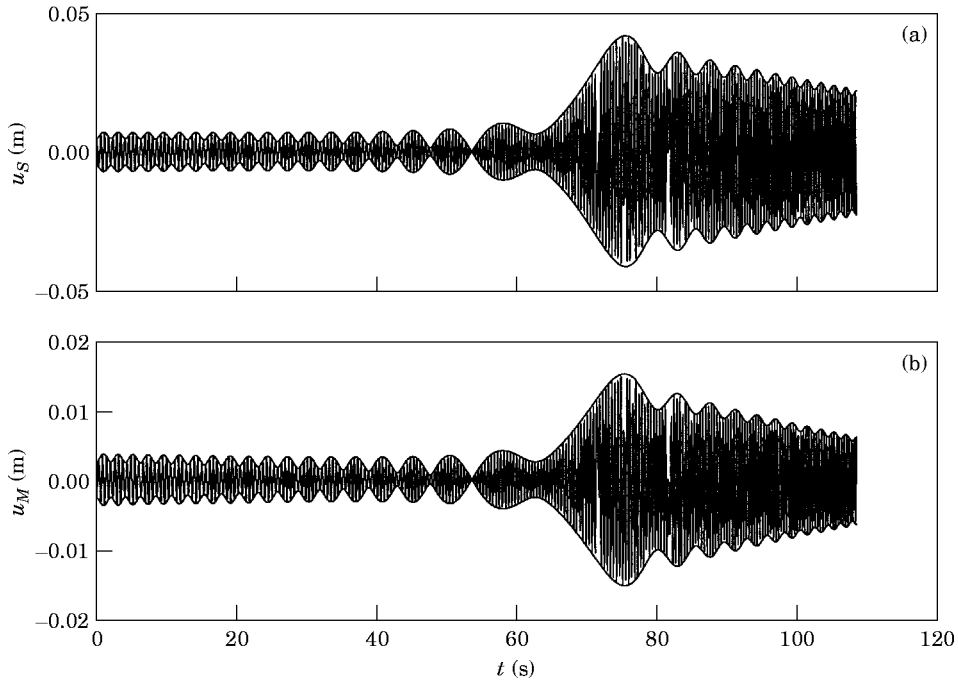

Figure 5. The time response of the system (a) at the sheave and (b) at the conveyance, for the winding velocity $v_c = 15$ m/s.

where $T_c^i = (M + mL_v)g$ is the initial equilibrium tension, and the strain e is given by equation (30). The total vertical cable tensions are obtained from

$$T_v(s, t) = T^i + EA\varepsilon(s, t), \tag{78}$$

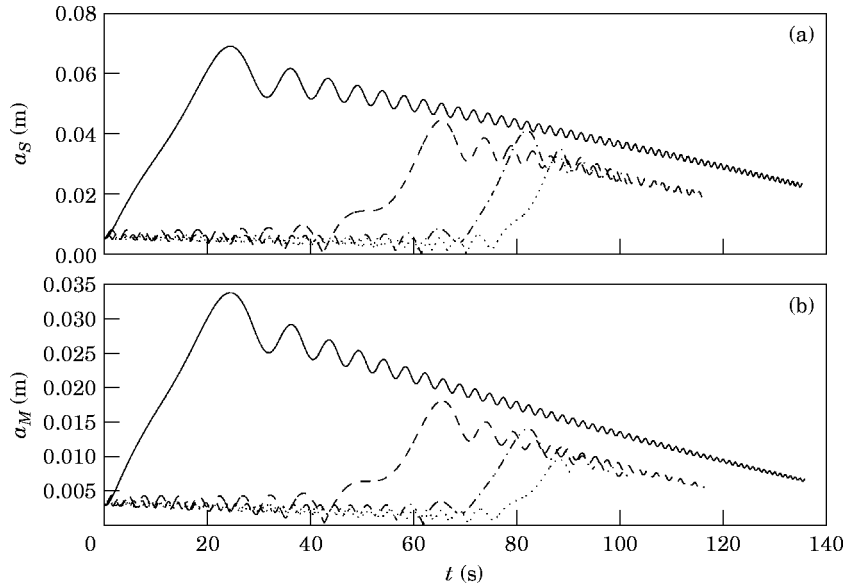

Figure 6. Vibration envelope curves (a) at the sheave and (b) at the conveyance, for the winding velocities $v_c = 12$ (——), 14 (– –), 16 (–·–) and 18 (···) m/s.

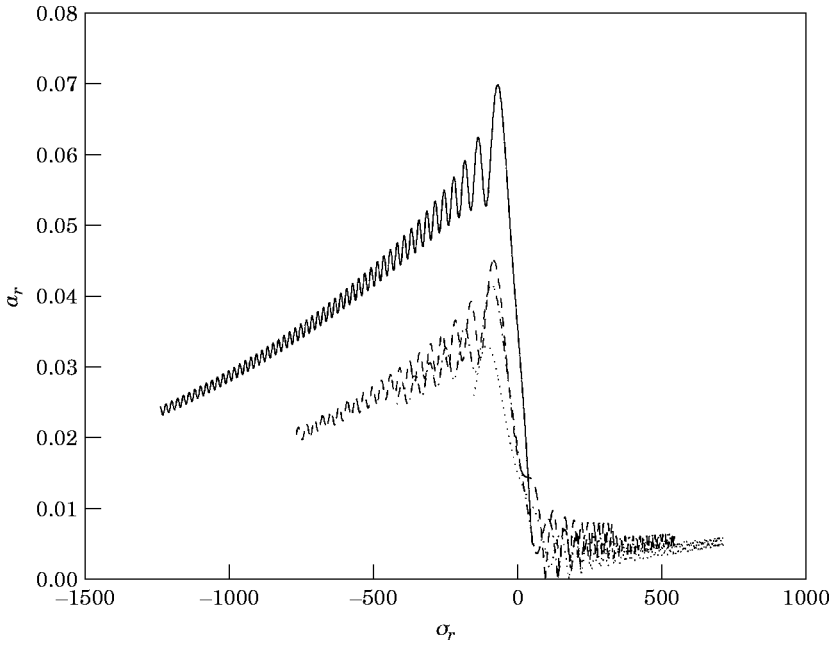

Figure 7. The non-stationary frequency–response curves for the winding velocities $v_c = 12$ (——), 14 (– –), 16 (–·–) and 18 (···) m/s.

where T^i is given by equation (42), and the strain ε is defined by equation (21), so that $T_S = T_v(L_1, t)$ and $T_M = T_v(L_0, t)$. It can be observed that the dynamic tension oscillates about the mean tension value, which for the catenary and at the sheave increases with the vertical length. The largest total tension is recorded in the catenary. The smallest tension

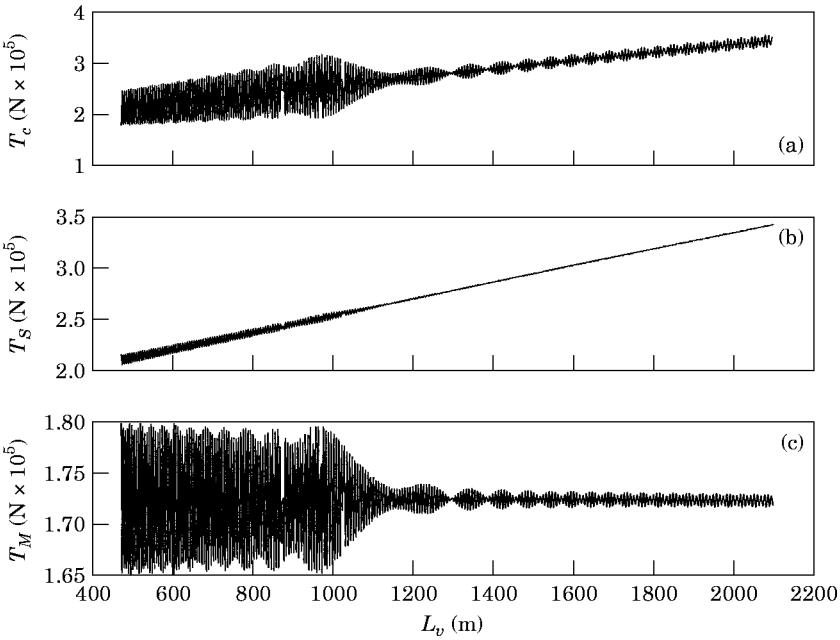

Figure 8. The total cable tensions at the winding velocity $v_c = 15$ m/s: (a) the the catenary tension T_c; (b) the vertical rope tension at the headsheave, T_S; (c) the vertical rope tension at the conveyance, T_M.

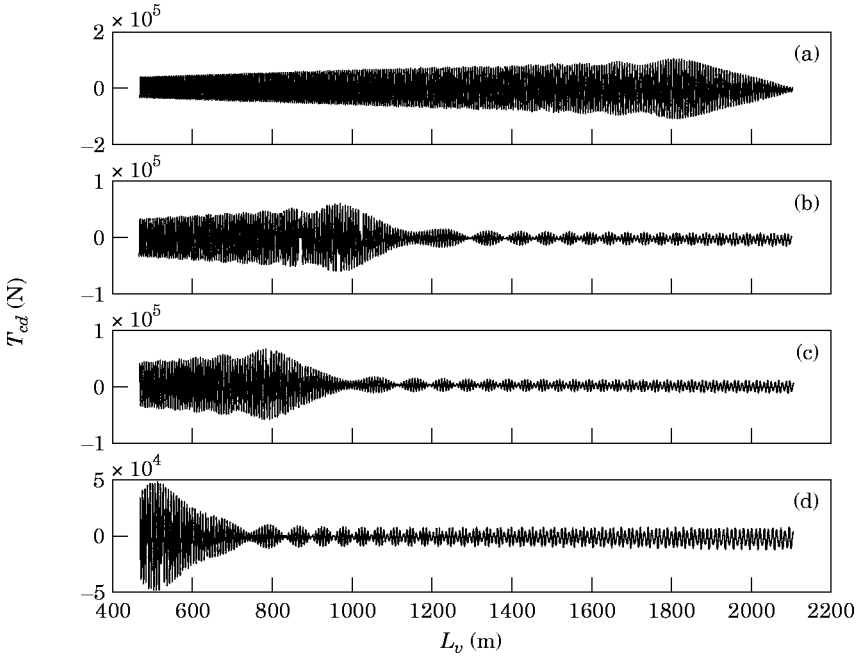

Figure 9. The dynamic catenary tensions for various winding velocities v_c: (a) 12, (b) 15, (c) 16 and (d) 18 m/s.

oscillations occur at the sheave, and the largest at the conveyance. As the tension oscillations contribute to fatigue damage of the cable it is of interest to examine the dynamic tension components in more detail. The dynamic catenary tension $T_{cd} = EAe$ for various values of the transport velocity are plotted against the vertical length in

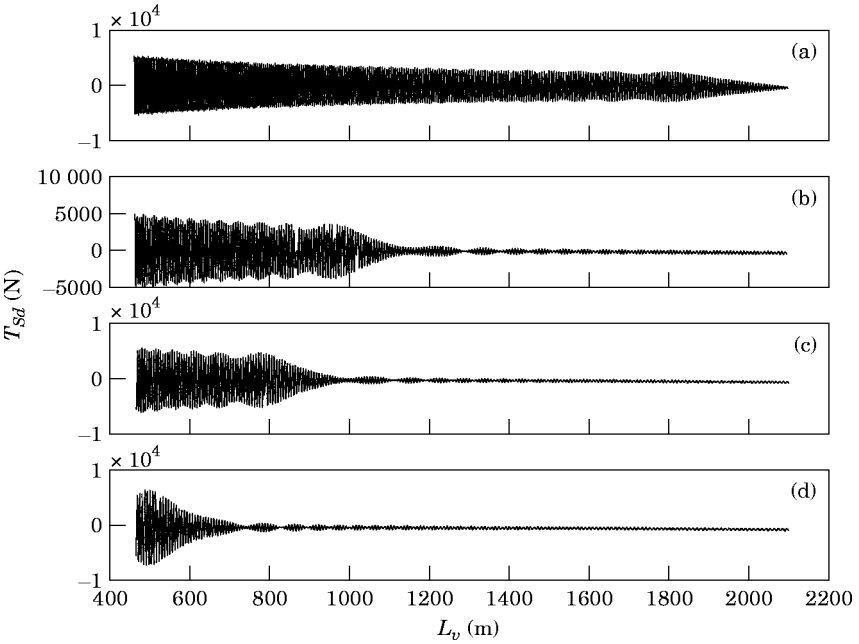

Figure 10. The dynamic vertical rope tensions at the headsheave for various winding velocities v_c: (a) 12, (b) 15, (c) 16 and (d) 18 m/s.

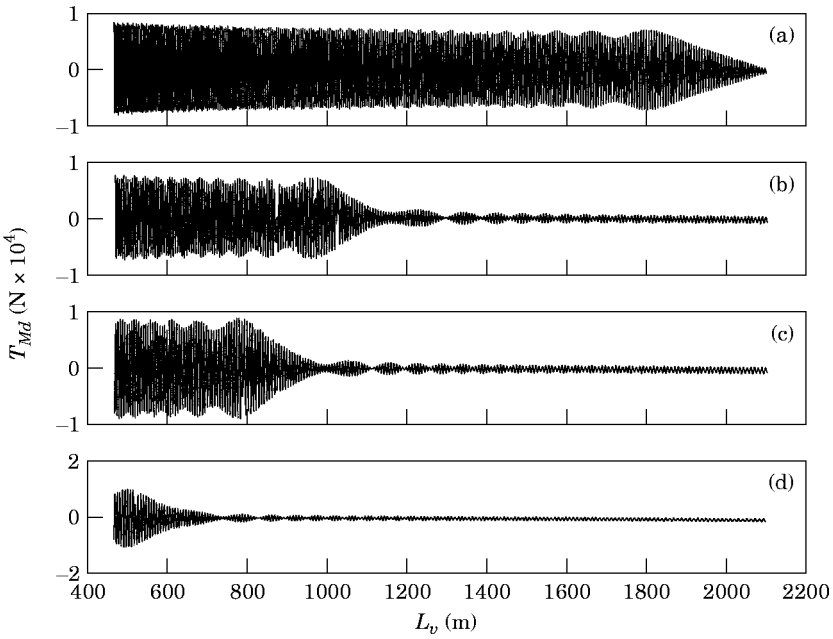

Figure 11. The dynamic vertical rope tensions at the conveyance for various winding velocities v_c: (a) 12, (b) 15, (c) 16 and (d) 18 m/s.

Figure 9. The highest tensions occur at the resonance region, declining slowly afterwards. It can be seen that the more rapid the passage through resonance the smaller the maximum amplitude of the tension oscillations. A different trend can be detected for the dynamic tensions $T_{Sd} = EA\varepsilon(L_1, t)$ and $T_{Md} = EA\varepsilon(L_0, t)$, at the sheave and at the conveyance

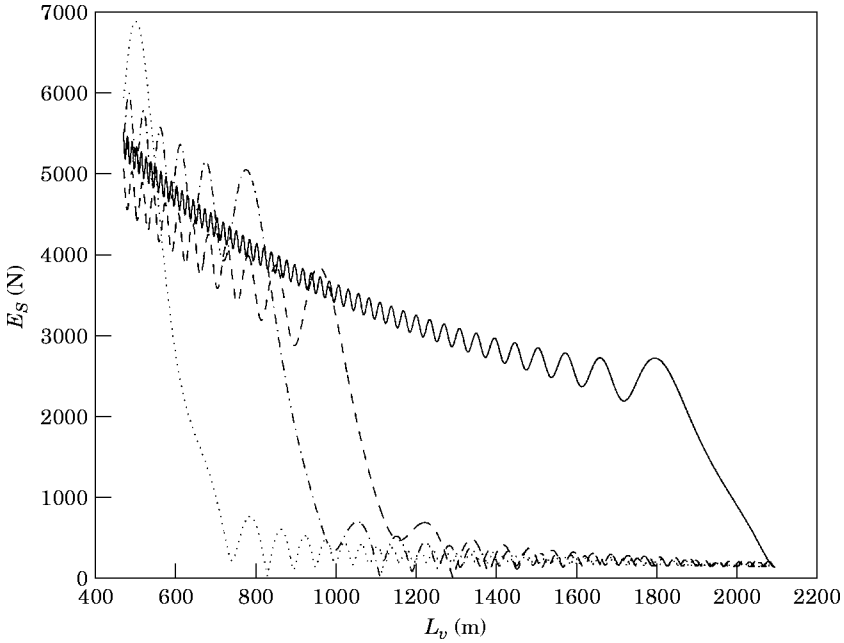

Figure 12. The sheave dynamic tension envelope curves for the winding velocities v_c = 12 (——), 15 (– –), 16 (–·–) and 18 (···) m/s.

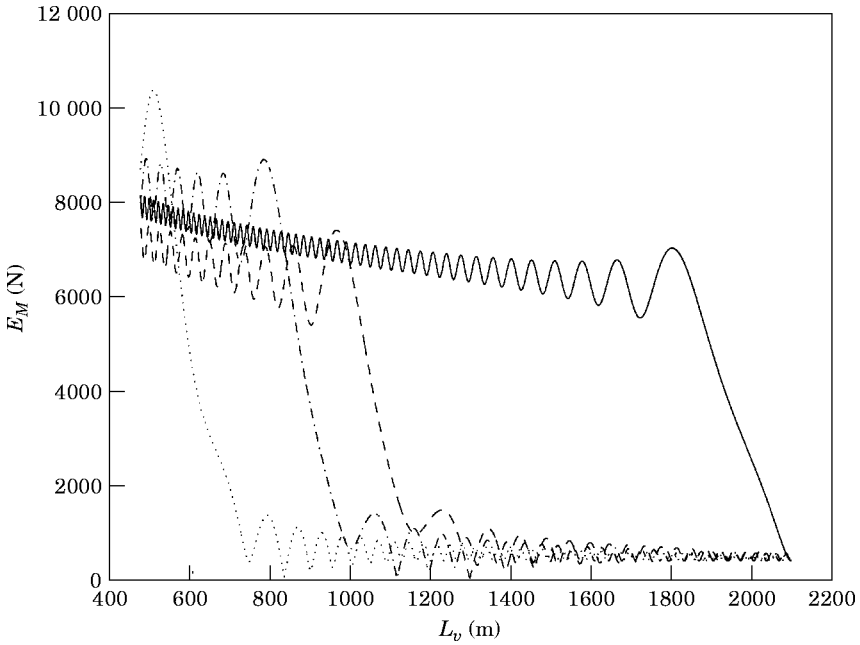

Figure 13. The conveyance dynamic tension envelope curves for the winding velocities $v_c = 12$ (——), 15 (—), 16 (–·–) and 18 (···) m/s.

respectively, which are shown in Figures 10 and 11. These tensions increase rapidly during the passage through resonance and continue to grow afterwards. It can be also noted that the amplitudes of the tension oscillations show the tendency to reach higher values for higher velocities, which can be better observed in Figures 12 and 13, where the sheave tension and the conveyance tension upper envelopes, determined as $E_S = EA(\partial Y_r/\partial s)(L_1, l)a_r$ and $E_M = EA(\partial Y_r/\partial s)(L_0, l)a_r$ respectively, are shown.

In order to integrate the equations (75) the initial conditions need to be specified. For example, these initial conditions are assumed as $a_r(0) = 0{\cdot}005$, and $\psi_r(0) = 0$ in the computations discussed. It is explained in detail in Appendix E how these initial values can be related to the initial conditions $q_r(0)$, $(\mathrm{d}_{q_r}/\mathrm{d}T)(0)$, and to $u(s, 0)$, and $\dot{u}(s, 0)$, respectively. As the system (57) is essentially linear, with slowly varying parameters however (therefore referred to as a quasi-linear system [10]), the initial conditions do not play a crucial role in the stability of motions of the system. In general, they are responsible for the transient part of the total response, and have little effect on the system behavior and on the amplitude during the passage through the resonance. This is demonstrated in Figure 14, where the amplitude–time curves for various initial values $a_r(0)$ are shown.

The accuracy of the first approximation (76), where a_r and ψ_r are given by equations (75), can be verified by numerically integrating the original differential equation (57) derived via the Rayleigh–Ritz procedure. The solution for q_r with the winding velocity $v_c = 15$ m/s, obtained through a numerical integration of equation (57), with superimposed envelopes formed by the amplitude curves calculated from the multiple scales model (75) is shown in Figure 15. It can be seen that the results correlate very well.

8. CONCLUSIONS

In slowly varying oscillatory systems, a transient resonance may take place if an external periodic excitation is present. For example, in a hoisting cable system the natural

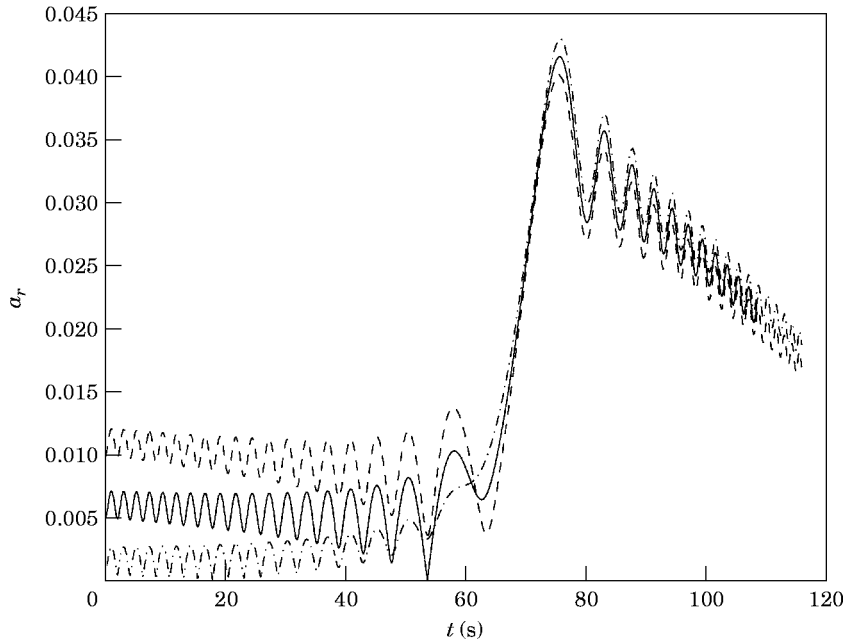

Figure 14. The amplitude–time curves for various initial values $a_r(0) = 0{\cdot}01$ (—), $0{\cdot}005$ (——) and $0{\cdot}0005$ (–·–), with $\psi_r(0) = 0$.

frequencies and mode shapes vary slowly during a winding cycle, and when the frequency of the excitation due to a coiling mechanism at the winding drum coincides with one of the natural frequencies a passage through resonance occurs. Perturbation techniques can be employed to analyze transient resonance in systems with slowly varying frequencies.

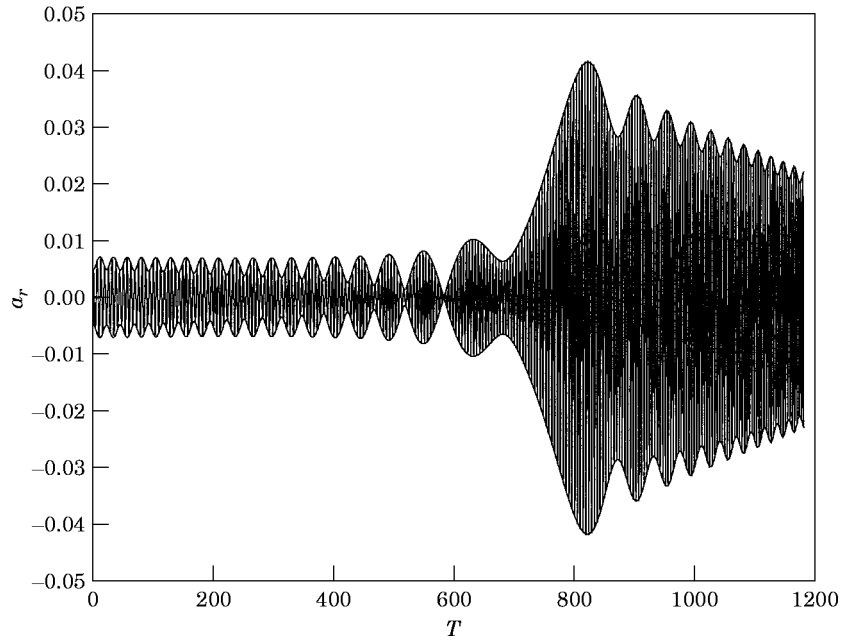

Figure 15. The numerical solution q_r with superimposed amplitude envelope curves obtained from the multiple scales system, at the winding velocity $v_c = 15$ m/s.

When combined with standard numerical integration methods, these techniques yield quick and accurate results even when long time intervals are involved.

This has been demonstrated for a single-mode model of a hoisting cable system. This simplified model forms essentially a single-degree-of-freedom approximation of the system. It accommodates the fundamental feature of the system, namely its non-stationary nature, and adequately represents the main type of vibration occurring in the system. The multiple scales method is used, which leads to a system of first order ordinary differential equations for the amplitude and phase of the response. These are slowly varying functions and the system can be solved numerically without difficulty. On the other hand, the direct integration procedure of the original second order differential equations of motion is very time-consuming. For example, to solve the problem for a typical industrial installation, with the parameters defined in the preceding section, in the interval $\tau \in [0{\cdot}0, 0{\cdot}75]$ for a value of $v_c = 14$ m/s, with a corresponding value of the small parameter $\varepsilon = 5{\cdot}9112 \times 10^{-4}$, requires an integration to a time of 1268·8 on the non-dimensional fast time scale T, and involves integrating a rapidly oscillating function that may yield inaccurate results.

The results obtained for the model example demonstrate the dynamic behavior of the hoisting system during a passage through resonance. The amplitude time plots and the non-stationary frequency–response curves for various winding velocities show that the more rapid the passage through resonance is, the smaller are the maxima of the response amplitudes, as for the shorter passage time intervals the development of resonance phenomena is restricted. This would indicate that if at some stage of the wind resonance is expected, higher winding velocities should be applied.

The highest maximum tension in the cable occurs in the catenary and at the sheave, when the payload is hoisted from the bottom position. The mean values of the catenary and of the sheave tension decrease during the ascent. In the resonance region substantial oscillations in the catenary and at the conveyance tension are recorded. In the catenary these oscillations decrease after the resonance, with decreasing vertical length. At the conveyance the tension oscillations continue to grow after the resonance.

Higher winding velocities limit oscillations in the dynamic catenary tension. However, it has been shown that the amplitudes of the vertical cable tension oscillations tend to reach larger values for higher velocities. This fact cannot be ignored, as high amplitude oscillations in the tension contribute directly to fatigue of the cable.

ACKNOWLEDGMENT

The author gratefully acknowledges the support received from the University of Natal Research Fund.

REFERENCES

1. G. N. Savin and O. A. Goroshko 1962 *The Dynamics of Threads with Variable Length* (*Applications in Mine Hoist Systems*). Kiev: The Ukrainian Academy of Sciences (in Russian).
2. G. N. Savin and O. A. Goroshko 1971 *Introduction to Mechanics of One-Dimensional Bodies with Variable Length*. Kiev: Naukova Dumka (in Russian).
3. T. Kotera 1978 *Bulletin of the Japan Society of Mechanical Engineers* **21**, 1469–1474. Vibrations of string with time-varying length.
4. M. E. Greenway 1989 *Internal Report*, *Anglo American Corporation*, *Johannesburg*, *South Africa*. Dynamic loads in winding ropes—an analytical approach.
5. R. R. Mankowski 1982 *Ph.D. Thesis*, *Department of Mechanical Engineering*, *University of the Witwatersrand*, *South Africa*. A study of nonlinear vibrations occurring in mine hoisting cables.

6. C. P. Constancon 1993 *Ph.D. Thesis*, *Department of the Mechanical Engineering*, *University of the Witwatersrand*, *South Africa*. The dynamics of mine hoist catenaries.
7. A. Kumaniecka and J. Niziol 1994 *Journal of Sound and Vibration* **178**, 211–226. Dynamic stability of a rope with slow variability of the parameters.
8. Y. A. Mitropolsky 1965 *Problems of the Asymptotic Theory in Nonstationary Vibrations*. Jerusalem: Israel Program for Scientific Translations.
9. B. N. Agrawal and R. M. Evan-Iwanowski 1973 *American Institute of Aeronautics and Astronautics Journal* **11**, 907–912. Resonances in nonstationary, nonlinear, multidegree-of-freedom systems.
10. R. M. Evan-Iwanowski 1976 *Resonance Oscillations in Mechanical Systems*. Amsterdam: Elsevier.
11. A. H. Nayfeh 1973 *Perturbation Methods*. New York: John Wiley.
12. J. Kevorkian 1971 *SIAM Journal of Applied Mathematics* **20**, 364–373. Passage through resonance for a one-dimensional oscillator with slowly varying frequency.
13. J. Kevorkian 1987 *SIAM Review* **29**, 391–461. Perturbation techniques for oscillatory systems with slowly varying coefficients.
14. D. L. Bosley and J. Kevorkian 1992 *SIAM Journal of Applied Mathematics* **52**, 494–527. Adiabatic invariance and transient resonance in very slowly varying oscillatory Hamiltonian systems.
15. A. H. Nayfeh and D. T. Mook 1979 *Nonlinear Oscillations*. New York: John Wiley.
16. J. G. de Jalon and E. Bayo 1994 *Kinematic and Dynamic Simulation of Multibody Systems*. New York: Springer-Verlag.
17. N. C. Perkins and C. D. Mote, Jr. 1987 *Journal of Sound and Vibration* **114**, 325–340. Three-dimensional vibration of travelling elastic cable.
18. S. Timoshenko, D. H. Young and W. Weaver 1974 *Vibration Problems in Engineering*. New York: John Wiley; fourth edition.
19. H. H. Vanderveldt, B. S Chung and W. T. Reader 1973 *Experimental Mechanics* **13**, 24–30. Some dynamic properties of axially loaded wire ropes.
20. G. R. Thomas and R. D. Brillhart 1987 *Final Report on an Investigation into the Dynamic Rope Loads in Drum Winder Systems*. San Diego, California: SDRC Inc.
21. R. R. Mankowski and F. J. Cox 1986 *Journal of the South African Institute of Mining and Metallurgy* **86**, 51–60. Response of mine hoisting cables to longitudinal shock loads.
22. H. H. Vanderveldt and J. J. Gilheany 1970 *Experimental Mechanics* **10**, 401–407. Propagation of a longitudinal pulse in wire ropes under axial loads.
23. W. Szemplinska-Stupnicka 1990 *The Behavior of Nonlinear Vibrating Systems*. Dordrecht: Kluwer.
24. C. Dimitriou and A. Whillier 1973 *SAIMechE Hoisting Conference*, *Johannesburg*, 16–20 *October* 1973. Vibrations in winding ropes: an appraisal.

APPENDIX A

The slowly varying coefficients appearing in the system (50) result from the application of the Rayleigh–Ritz method, and are defined as follows:

$$m_r(\tau) = \int_{L_1}^{L_0} \rho(s) Y_r^2 \, \mathrm{d}s, \quad b_{rr}(\tau) = \int_{L_1}^{L_0} \mu_1(s) Y_r \frac{\partial Y_{r,ss}}{\partial l} \, \mathrm{d}s, \quad c_{rr}(\tau) = \int_{L_1}^{L_0} \rho(s) Y_r \frac{\partial Y_r}{\partial l} \, \mathrm{d}s, \tag{A1–A3}$$

$$d_{rr}(\tau) = \int_{L_1}^{L_0} \rho(s) Y_r \frac{\partial Y_r^2}{\partial l^2} \, \mathrm{d}s, \quad e_r(\tau) = \int_{L_1}^{L_0} \rho(s) Y_r \, \mathrm{d}s, \quad g_{rr}(\tau) = \int_{L_1}^{L_0} \mu_1(s) Y_r Y_{r,ss} \, \mathrm{d}s, \tag{A4–A6}$$

where the mode function Y_r is defined by equation (46), and the partial derivatives of Y_r with respect to l are determined as follows:

$$\frac{\partial Y_r}{\partial l} = \left(\gamma_r - \frac{\mathrm{d}\gamma_r}{\mathrm{d}l} z\right)\left[\sin \gamma_r z + \frac{M_s}{m} \gamma_r \cos \gamma_r z\right] - \frac{M_s}{m} \frac{\mathrm{d}\gamma_r}{\mathrm{d}l} \sin \gamma_r z, \tag{A7}$$

$$\frac{\partial^2 Y_r}{\partial l^2} = \left(2\frac{\mathrm{d}\gamma_r}{\mathrm{d}l} - \frac{\mathrm{d}^2\gamma_r}{\mathrm{d}l^2}z\right)\left[\sin\gamma_r z + \frac{M_s}{m}\gamma_r\cos\gamma_r z\right]$$

$$+ \frac{M_s}{m}\left(\gamma_r - \frac{\mathrm{d}\gamma_r}{\mathrm{d}l}z\right)\left[2\frac{\mathrm{d}\gamma_r}{\mathrm{d}l}\cos\gamma_r z - \gamma_r\left(\frac{\mathrm{d}\gamma_r}{\mathrm{d}l}z - \gamma_r\right)\sin\gamma_r z\right]$$

$$- \left(\gamma_r - \frac{\mathrm{d}\gamma_r}{\mathrm{d}l}z\right)^2\cos\gamma_r z - \frac{M_s}{m}\frac{\mathrm{d}^2\gamma_r}{\mathrm{d}l^2}\sin\gamma_r z. \tag{A8}$$

The derivatives of the eigenvalue γ_r with respect to l are obtained through differentiation of the frequency equation (47), which yields

$$\mathrm{d}\gamma_r/\mathrm{d}l = N_r(l)/D_r(l), \tag{A9}$$

where

$$N_r = \gamma_r\left[\left(1 - \frac{M_s M}{m^2}\gamma_r^2\right)\cos\gamma_r L_v - \frac{M_s + M}{m}\gamma_r\sin\gamma_r L_v\right], \tag{A10}$$

$$D_r = \left[\frac{M_s + M}{m} + L_v\left(1 - \frac{M_s M}{m^2}\gamma_r^2\right)\right]\cos\gamma_r L_v - \left(2\frac{M_s M}{m^2} + L_v\frac{M_s + M}{m}\right)\gamma_r\sin\gamma_r L_v, \tag{A11}$$

and

$$\frac{\mathrm{d}^2\gamma_r}{\mathrm{d}l^2} = \frac{1}{D_r^2}\left(\frac{\mathrm{d}N_r}{\mathrm{d}l}D_r - N_r\frac{\mathrm{d}D_r}{\mathrm{d}l}\right). \tag{A12}$$

APPENDIX B

The method of multiple scales is employed to find the solution of equation (57). This solution is sought in the form of expansion (59) with the slow time scale τ, and the fast scale ϕ_r defined by equation (60). It follows that the derivatives of the generalized co-ordinate q_r with respect to T become expansions in terms of the partial derivatives with respect to these variables:

$$\frac{\mathrm{d}q_r}{\mathrm{d}T} = \tilde{\omega}_r\frac{\partial q_r}{\partial\phi_r} + \varepsilon\frac{\partial p_r}{\partial\tau}, \tag{B1}$$

$$\frac{\mathrm{d}^2 q_r}{\mathrm{d}T^2} = \tilde{\omega}_r^2\frac{\partial^2 q_r}{\partial\phi_r^2} + \varepsilon\left(2\tilde{\omega}_r\frac{\partial^2 q_r}{\partial\phi_r\,\partial\tau} + \tilde{\omega}_r'\frac{\partial q_r}{\partial\phi_r}\right) + \varepsilon^2\frac{\partial^2 q_r}{\partial_\tau^2}, \tag{B2}$$

where the prime denotes the derivative with respect to τ. Hence equation (57) becomes

$$\tilde{\omega}_r^2\frac{\partial^2 q_r}{\partial\phi_r^2} + \varepsilon\left(2\tilde{\omega}_r\frac{\partial^2 q_r}{\partial\phi_r\,\partial r} + \tilde{\omega}_r'\frac{\partial q_r}{\partial\phi_r}\right) + \varepsilon^2\frac{\partial^2 q_r}{\partial\tau^2} + \tilde{\omega}_r^2 q_r$$

$$= \varepsilon f_r\left(\tau, \tilde{\omega}_r\frac{\partial q_r}{\partial\phi_r} + \varepsilon\frac{\partial q_r}{\partial_\tau}\right) + K_r\cos\tilde{\Omega}T + O(\varepsilon^2). \tag{B3}$$

Substituting (59) into (B3) with K_r represented by (64), and equating coefficients of like powers of ε, the system (65–66) is obtained.

APPENDIX C

The slowly varying frequency in the system (57) is given by

$$\tilde{\omega}_r = \bar{\omega}_r/\bar{\omega}_0, \tag{C1}$$

where

$$\bar{\omega}_r = \sqrt{\omega_r^2(l(\tau)) + \frac{1}{m_r(l(\tau))}\frac{EA}{L_c}}\,. \tag{C2}$$

Its derivative with respect to τ is

$$\tilde{\omega}_r' = (l'/\bar{\omega}_0)\,\mathrm{d}\bar{\omega}_r/\mathrm{d}l, \tag{C3}$$

where

$$\frac{\mathrm{d}\bar{\omega}_r}{\mathrm{d}l} = \frac{1}{2\sqrt{\omega_r^2 + \dfrac{1}{m_r}\dfrac{EA}{L_c}}}\left(2c\omega_r\frac{\mathrm{d}\gamma_r}{\mathrm{d}l} - \frac{EA}{m_r^2 L_c}\,\mathrm{d}m_r/\mathrm{d}l\right), \tag{C4}$$

with $\mathrm{d}\gamma_r/\mathrm{d}l$ given by equation (A9), and with $\mathrm{d}m_r/\mathrm{d}l$ being determined from equation (A1) as

$$\frac{\mathrm{d}m_r}{\mathrm{d}l} = m\left[2\int_{L_1}^{L_0} Y_r(s, l)\frac{\partial Y_r}{\partial l}(s, l)\,\mathrm{d}s - 1\right] + 2MY_r(L_0, l)\frac{\partial Y_r}{\partial l}(L_0, l), \tag{C5}$$

where $\partial Y_r/\partial l$ is given by equation (A7).

APPENDIX D

The differential equation for the stationary free longitudinal motion of the unconstrained system shown in Figure 3 can be written as

$$\ddot{u} - c^2 u_{,zz} = 0, \tag{D1}$$

which must be satisfied over the domain $0 < z < L_v$, and where $z = s - L_1$. In addition, u must satisfy the boundary conditions

$$M_S\ddot{u}(0, t) - EAu_{,z}(0, t) = 0, \qquad M\ddot{u}(L_v, t) + EAu_{,z}(L_v, t) = 0. \tag{D2, D3}$$

By using the separation of variables method, the displacement u is expressed as

$$u(z, t) = Y(z)f(t), \tag{D4}$$

where f is an harmonic function of time with the frequency ω, so that $\ddot{u} = -\omega^2 Y(z)f(t)$. The eigenvalue problem (D1–D3) is then reduced to

$$\mathrm{d}^2 Y/\mathrm{d}z^2 + \gamma^2 Y = 0, \tag{D5}$$

with the boundary conditions in the form

$$M_S\omega^2 Y(0) + EA\frac{\mathrm{d}Y}{\mathrm{d}z}(0) = 0, \qquad -M_S\omega^2 Y(L_v) + EA\frac{\mathrm{d}Y}{\mathrm{d}z}(L_v) = 0. \quad \text{(D6, D7)}$$

The solution of equation (D5) is

$$Y(z) = C\cos\gamma z + D\sin\gamma z, \tag{D8}$$

so that the conditions (D6 and D7) yield

$$\begin{bmatrix} -M_S\omega^2 & -EA\gamma \\ -(M\omega^2\cos\gamma L_v + EA\gamma\sin\gamma L_v) & EA\gamma\cos\gamma L_v - M\omega^2\sin\gamma L_v \end{bmatrix}\begin{bmatrix} C \\ D \end{bmatrix} = 0. \tag{D9}$$

Therefore, a non-trivial solution is possible only if the determinant of the coefficient matrix in equation (D9) vanishes, which results in the following:

$$\frac{M_S}{m}\gamma\left(\cos\gamma L_v - \frac{M}{m}\gamma\sin\gamma L_v\right) + \frac{M}{m}\gamma\cos\gamma L_v + \sin\gamma L_v = 0, \tag{D10}$$

or $\gamma = 0$ (a rigid-body mode). For the non-zero eigenvalues γ, the eigenfunction and coefficients C and D can be obtained from equation (D9). Upon scaling $C = 1$, the elastic mode shapes are given as

$$Y_n = \cos\gamma_n z - (M_S/m)\gamma_n\sin\gamma_n z. \tag{D11}$$

APPENDIX E

In order to integrate the system (75) to determine the slowly varying amplitude a_r and phase ψ_r initial conditions have to be specified. It remains to show how the initial amplitude $a_r(0)$ and the initial phase $\psi_r(0)$ are related to the initial conditions corresponding to the original partial differential equation system (44). These initial conditions can be stated as

$$u(s, 0) = \varphi_1(s), \qquad \dot{u}(s, 0) = \varphi_2(s), \tag{E1}$$

where φ_1 and φ_2 are prescribed functions. Upon the representation (45), and assuming $\dot{l}(0) = 0$, these conditions result in the forms

$$Y_r(s, l(0))q_r(0) = \varphi_1(s), \qquad Y_r(s, l(0))\dot{q}_r(0) = \varphi_2(s). \quad \text{(E2, E3)}$$

Multiplying equations (E2) and (E3) by $\rho(s)Y_r(s, l(0))$, and integrating the results from $L_1(0)$ to L_0 yields the initial values of q_r and $\dot{q}_r$ as

$$q_r(0) = \frac{1}{m_r(l(0))}\int_{L_1(0)}^{L_0}\rho(s)Y_r(s, l(0))\varphi_1(s)\,\mathrm{d}s, \tag{E4}$$

$$\dot{q}_r(0) = \frac{1}{m_r(l(0))}\int_{L_1(0)}^{L_0}\rho(s)Y_r(s, l(0))\varphi_2(s)\,\mathrm{d}s. \tag{E5}$$

When the non-dimensional time scale T is introduced by (53), the initial value for $\mathrm{d}q_r/\mathrm{d}T$ is given as

$$\frac{\mathrm{d}q_r}{\mathrm{d}T}(0) = \frac{1}{\bar{\omega}_0}\dot{q}_r(0). \tag{E6}$$

The first approximation to the solution of equation (57) is given by equation (67). This approximation can also be written in the form

$$q_r = C_{r1}(\tau)\cos\phi_r + C_{r2}\sin\phi_r + O(\varepsilon), \tag{E7}$$

where the slowly varying parameters C_{r1} and C_{r2} are related to the amplitude a_r and the phase β_r by

$$a_r = \sqrt{C_{r1}^2 + C_{r2}^2}, \qquad \beta_r = \tan^{-1}(-C_{r2}/C_{r1}). \tag{E8}$$

Noting that $\phi_r = \int_0^T \bar{\omega}_r(\varepsilon\xi)\,\mathrm{d}\xi$, and taking into consideration that

$$\frac{\mathrm{d}q_r}{\mathrm{d}T} = \bar{\omega}_r(-C_{r1}\sin\phi_r + C_{r2}\cos\phi_r) + O(\varepsilon), \tag{E9}$$

yields the results

$$q_r(0) = C_{r1}(0) + O(\varepsilon), \qquad \frac{\mathrm{d}q_r}{\mathrm{d}T}(0) = \bar{\omega}_0 C_{r2} + O(\varepsilon). \tag{E10}$$

Therefore, disregarding the terms $O(\varepsilon)$ and combining equations (E10) and (E8), yields initial values for a_r and β_r, to first order approximation:

$$a_r(0) = \sqrt{q_r^2(0) + \left[\frac{1}{\bar{\omega}_0}\frac{\mathrm{d}q_r}{\mathrm{d}T}(0)\right]^2}, \qquad \beta_r(0) = \tan^{-1}\left(\frac{-1}{\bar{\omega}_0 q_r(0)}\frac{\mathrm{d}q_r}{\mathrm{d}T}(0)\right), \tag{E11, E12}$$

where $q_r(0)$ and $(\mathrm{d}q_r/\mathrm{d}T)(0)$ are determined from equations (E4–E6). Using equation (73) together with equation (63) yields the initial phase ψ_r as

$$\psi_r(0) = -\beta_r(0). \tag{E13}$$

For example, it can be found from equations (E11–E13) that the initial conditions $a_r(0) = 0{\cdot}005$, $\psi_r(0) = 0$ correspond to $q_r(0) = 0{\cdot}005$ and $(\mathrm{d}q_r/\mathrm{d}T)(0) = 0$. Therefore, for the parameter set used in the model example of section 7, this would give the initial displacements at the sheave, and at the conveyance as $u_1(0) = 0{\cdot}005$ m, and $u_2(0) = -0{\cdot}0026$ m, respectively, with $\dot{u}(s, 0) = 0$.